Searching for new physics in two-body decays: Ideas and pitfalls

E. Arrieta Diaz[1], *F. Benitez*[2], *A. Büchler*[3], *L.J. Cieri*[4], *A. Florez*[5], *E. Garces-Garcia*[6], *B. Gonçalves*[7], *F. Koetsveld*[8], *K.J.C. Leney*[9], *H. Marquez Falcon*[10], *M. Moncada*[11], *P. Quintero*[11], *D. Romero*[12], *K. Shaw*[13], *J. Swain*[14], *M.P. Zurita*[4]

[1] Michigan State University, East Lansing, Michigan, United States of America
[2] Universidad de la República, Montevideo, Uruguay
[3] Universität Zürich, Zurich, Switzerland
[4] Universidad de Buenos Aires, Buenos Aires, Argentina
[5] Vanderbilt University, Nashville, Tenessee, United States of America
[6] Dpto. de Física, CINVESTAV, México DF, Mexico
[7] Universidade Federal de Juiz de Fora, Juiz de Fora, Brazil
[8] Nikhef, Radboud Universiteit, Nijmegen, Netherlands
[9] University of Liverpool, Liverpool, United Kingdom
[10] Universidad Michoacana de San Nicolás de Hidalgo, Morelia, Mexico
[11] Universidad Nacional de Colombia, Bogotá, Colombia
[12] Pontificia Universidad Católica de Chile, Santiago, Chile
[13] University of Sheffield, Sheffield, United Kingdom
[14] Northeastern University, Boston, Massachussets, United States of America

Abstract

Many new physics processes, and indeed many Standard Model interactions involve two-body decays. Although the kinematics are relatively simple, mistakes can easily be made when applying cuts to data in order to separate the signal from backgrounds. We present a short, but relevant list of possible sources of errors, and discuss the consequences of these.

A copy of the slides presented during the oral report at the school can be found at the URL below
`http://cern.ch/PhysicSchool/LatAmSchool/2009/Presentations/pDG3.pdf`

1 Introduction

There are many interesting two-body decay processes, including those by which the existence of the Higgs boson could be confirmed or denied, or where an indication of new physics processes (beyond the Standard Model) are expected to appear. There are, however, several problems associated with the analysis of this type of process, which are rarely documented. These mostly stem from the fact that once cuts start to be made on kinematic variables (for example transverse momentum or pseudo-rapidity of the decay particles), one may be over-constraining the kinematics, thus biasing the experimental data.

The kinematics of two-body decay processes are covered in Section 2, followed by two examples of possible actual processes — $B_S \to \mu^+\mu^-$ and $H \to ZZ^* \to 4$ leptons — both of which will be well within the reach of the LHC, which is due to start taking data in November 2009. The former is the experimentally simpler of the two analyses, since the final state simply consists of two muons, and the mass of the B_S is well known from data. The Higgs analysis is complicated by the fact that not only is the mass of the Higgs unknown, but also that the two Z bosons themselves subsequently decay, leaving four particles in the final state.

Finally, a summary of some of the general problems and common mistakes associated with two-body decay analyses is made in Section 6, together with examples of common cuts which can adversely affect the experimental results.

2 General kinematics

The general kinematics of two-body decay processes of the type $A \to B + C$ are best described in the centre-of-mass frame, where the decaying particle (A) is at rest. Conservation of 4-momentum implies that B and C are emitted back-to-back, with their 3-momenta being equal and opposite. Furthermore, Lorentz invariance implies no preferred direction for the final 3-momenta, which is reflected in the absence of angular dependence in the kinematics. The initial 4-momentum can then be written in the form

$$p_A = (m_A, \overrightarrow{0}).$$

The quantity p_A is of course conserved, being equal to the sum of the final momenta p_B and p_C, where

$$p_B = (E_B, \overrightarrow{p_B}) \qquad\qquad p_C = (E_C, \overrightarrow{p_C}) \tag{1}$$

with $\overrightarrow{p_B} = -\overrightarrow{p_C} = \overrightarrow{p}$. It can then easily be shown that the energies and absolute values of the final 3-momenta of B and C can be expressed in terms of only the invariant masses of the particles.

$$\begin{aligned} E_B &= \frac{m_A^2 + m_B^2 - m_C^2}{2m_A} \\ E_C &= \frac{m_A^2 - m_B^2 + m_C^2}{2m_A} \end{aligned} \tag{2}$$

and

$$|\overrightarrow{p}| = \sqrt{E_B^2 - m_B^2} = \frac{m_A^2 - (m_B^2 + m_C^2)}{2m_A}. \tag{3}$$

3 Phase space

The phase space for two-body decays is severely constrained, which makes these types of decay conceptually easy to treat. Here, we analyse the basic kinematics in the general case. The differential decay rate of an unstable particle to a given final state in the centre-of-mass frame is [1]

$$d\Gamma = \frac{1}{2m_A}\left(\Pi_f \frac{d^3p_f}{(2\pi)^3}\frac{1}{2E_f}\right)|\mathcal{M}_{fA}|^2\,(2\pi)^4\delta^{(4)}(p_A - \sum p_f), \tag{4}$$

where the matrix element $\mathcal{M}_{fA}$ is the Feynman amplitude related to the quantum probability of the process, $2m_A$ is the incoming flux, E_f is the energy of the final-state particle (e.g., E_B, E_C), p_A is the 4-momentum of the decaying particle, p_f is the 4-momentum of the final-state particle (p_B, p_C), and the δ function accounts for 4-momentum conservation.

For the special case of a two-particle final state, the integration over the phase space takes the simpler form

$$\int \left(\Pi_f \frac{d^3p_f}{(2\pi)^3}\frac{1}{2E_f}\right)(2\pi)^4\delta^{(4)}(p_A - \sum p_f) = \int \frac{d\Omega_{CM}}{4\pi}\frac{1}{8\pi}\Big(\frac{2|\overrightarrow{p}|}{E_{CM}}\Big), \tag{5}$$

where $|\overrightarrow{p}|$ is the magnitude of the 3-momentum of either final particle. Finally, in the special case where particles B and C have the same mass, it can easily be shown that

$$\Gamma = \frac{1}{2m_A}\frac{1}{8\pi}\frac{2|\overrightarrow{p}|}{E_{CM}}\,|\mathcal{M}_{fA}|^2\ . \tag{6}$$

This expression shows that the phase space is severely constrained in the case of two-body decays. As will be shown below, this has to be taken into account at the time of performing background cuts to possible measurements.

The $|\mathcal{M}_{fA}|^2$ factor in all these expressions has to be supplemented by the actual physical process taking place, and can be computed using the relevant Feynman rules, as will be shown in the following two important examples.

4 $B_S \to \mu^+\mu^-$

b-quarks are bound by strong dynamics into colour-neutral hadrons, and the non-perturbative nature of these states makes the extraction of precision information about physics at high energies problematic. To explore possible new physics effects it is necessary to untangle them from non-perturbative QCD effects.

This is, as yet, an unsolved problem, and no unique solution exists. Instead, there are a variety of theoretical approaches and techniques, generally adapted to specific problems. While approaches based directly on QCD are clearly to be preferred, model-dependent methods are often the only option available and thus also play an important role. Effective field theories, such as the heavy-quark expansion or chiral perturbation theory are commonly used too.

These theories are based on the idea that in a given process only certain degrees of freedom may be relevant to understand the physics involved. This is often the case when kinematical considerations restrict the momenta of external particles, effectively constraining the momenta of virtual particles as well.

One can argue that in these cases it makes sense to remove from the theory all intermediate states of high virtuality. Their absence might be compensated for by introducing new (effective) interactions between the remaining degrees of freedom. Using this approach one can recover, for example, the Fermi theory of weak interactions at low energies; starting from the Standard Model Lagrangian and integrating out the massive gauge vectors.

What makes an effective field theory powerful is that the deviation from the limiting behaviour may be organized in a systematic expansion in a small parameter, usually related to the scale up to which the theory makes sense. An effective field theory is then predictive, precisely because it is under perturbative control.

Many quantities of experimental and phenomenological importance cannot be analysed by these methods, however, even if these are systematic and well understood. For the description of exclusive hadronic weak decays, most exclusive semi-leptonic decays, strong decays, fragmentation, and many other interesting aspects of B-physics, only a few model-dependent approaches are available.

4.1 Theoretical framework

The decays $B^0_{s,d} \to l^+l^-$ are dominated by the Z^0 penguin (also called vertical or annihilation penguin) and box diagrams involving top quark exchanges, as shown in Fig. 1.

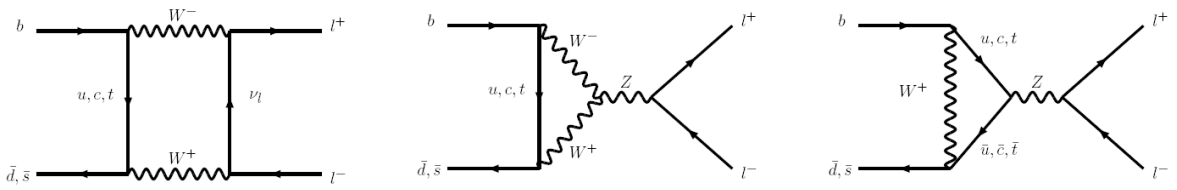

Fig. 1: Decay processes contributing to $B^0_{s,d} \to l^+l^-$ in the Standard Model

The effective Hamiltonian for $B^0_{s,d} \to l^+l^-$ decays is given by

$$H_{eff} = -\frac{4G_f}{\sqrt{2}} V_{tb}^* V_{tq} \left[C_{10} Q_{10} + C_S Q_S + C_P Q_P \right] \ , \tag{7}$$

where q indicates a strange quark for the B_s^0 or a down quark in the case of the B_d^0.

$$Q_S = \frac{e^2}{16\pi^2} (\bar{q}_{L\alpha} b_{R\alpha})(\bar{l}l)$$
$$Q_P = \frac{e^2}{16\pi^2} (\bar{q}_{L\alpha} b_{R\alpha})(\bar{l}\gamma_5 l)$$

C_S and C_P are the Wilson coefficients for the Standard Model Higgs penguin, and the would-be neutral Goldstone boson penguin, respectively. However, these contributions to the amplitude are suppressed by a factor of m_b^2/M_W^2 relative to the main contribution and can be ignored (although it should be noted that C_S and C_P can become non-negligible for some extensions of the Standard Model). Thus, the Standard Model decay amplitude is given by the Wilson coefficient

$$C_{10} = -Y(x_t)/\sin^2\theta_W = -4.2 \ , \tag{8}$$

where

$$\begin{aligned} Y(x_t) &= \eta_\gamma \cdot Y_0(x_t) \\ Y_0(x_t) &= \frac{x}{8}\Big[\frac{x_t - 4}{x_t - 1} + \frac{3x_t}{(x_t-1)^2}\log x_t\Big] \\ x_t &= \frac{m_t^2}{M_W^2}. \end{aligned} \tag{9}$$

Here η_Y summarizes the next-to-leading-order correction with $\eta_Y = 1.012$. Evaluating the hadronic matrix element, the resulting branching ratio for $B_{q=s,d}$ is

$$\begin{aligned} \mathbf{B}(B_q \to l^+ l^-) = &\frac{G_F^2 \alpha^2 m_{B_q}^2 \tau_{B_q} f_{B_q}^2}{64\pi^3} \mid V_{tb}^* V_{tq} \mid^2 \sqrt{1 - \frac{4m_l^2}{m_{B_q}}} \\ &\times \left[\left(1 - \frac{4m_l^2}{m_{B_q}}\right) \mid \frac{m_{B_q}}{m_b + m_q} C_S \mid^2 + \mid \frac{2m_l}{m_{B_q}} C_{10} - \frac{m_{B_q}}{m_b + m_q} C_P \mid^2 \right], \end{aligned} \tag{10}$$

where τ_{B_q} signifies the B_q lifetime, and f_{B_q} is the B_q decay constant normalized according to $f_\pi = 132$ MeV. The Standard Model predictions are $BR(B_d^0 \to \mu^+\mu^-) = 1.02 \pm 0.09 \times 10^{-10}$, $BR(B_s^0 \to \mu^+\mu^-) = 3.37 \pm 0.31 \times 10^{-9}$ [2]. The 95% confidence level experimental limits by CDF are $B_d^0 \to \mu^+\mu^- < 3.0 \times 10^{-8}$ and $B_s^0 \to \mu^+\mu^- < 1.0 \times 10^{-7}$ [3].

4.2 Background

There are three main backgrounds to B_s production at the LHC [4]. Misidentified B-mesons provide the largest contribution, followed by combinatorics from di-muon events. The $B_c \to J/\Psi(\mu\mu)\mu\nu_\mu$ process (which passes the invariant mass cut because the B_c is slightly heavier than the B_s) is also significant. Provided the mass resolution of the detector is good enough, decays from other B-mesons can be safely ignored as background [4].

5 $H \to ZZ^* \to 4$ leptons

The search for the Higgs boson will be one of the primary tasks of the LHC and it has been established by many studies [5] that a Standard Model Higgs boson can be discovered with high significance at the LHC, over the full range of mass interest, from the lower limit of 114 GeV up to about 1 TeV.

The predominant Higgs production mechanism at the LHC will be gluon–gluon fusion, accounting for approximately 80% of all events (dependent on the Higgs mass). The second largest contribution comes from the fusion of vector bosons radiated from the initial-state quarks [5]. Production cross-sections as a function of Higgs mass are shown in Fig. 2 [6].

The $H \to \gamma\gamma$ channel looks to be a promising channel for Higgs masses less than 140 GeV, while for heavier Higgses the most promising searches involve decays to pairs of vector bosons (W^+W^-, ZZ). The only direct fermion decays with significant branching ratios are to $b\bar{b}$ and to two tau leptons. These are particularly important channels for a measurement of the Higgs boson coupling to fermions.

For $M_H > 125$ GeV, the four-lepton decay from $H \to ZZ^*$ provides a very clean signature over a wide mass range (up to 600 GeV) thanks to a combination of a narrow reconstructed mass peak and relatively low backgrounds. This is particularly true when $M_H > 180$ GeV, where the cross-section for two on-shell Z bosons opens up.

Furthermore, the $H \to ZZ^* \to 4l$ channel is also interesting because it allows for measurements of the spin of the Higgs to be made, through observations of the angle between pairs of leptons.

The branching ratios for these main decays as a function of Higgs mass are shown in Fig. 3 [6].

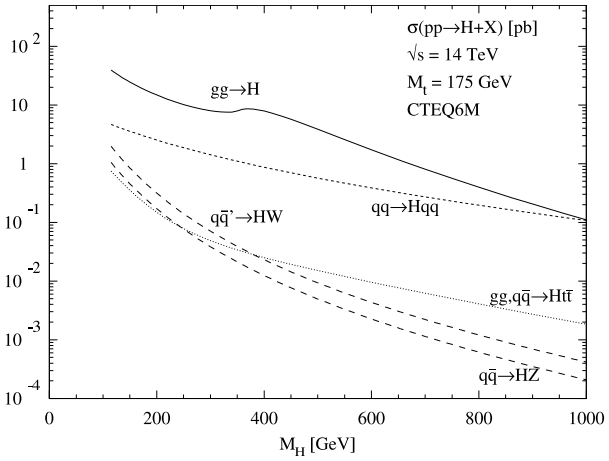

Fig. 2: Higgs production cross-section as a function of M_H

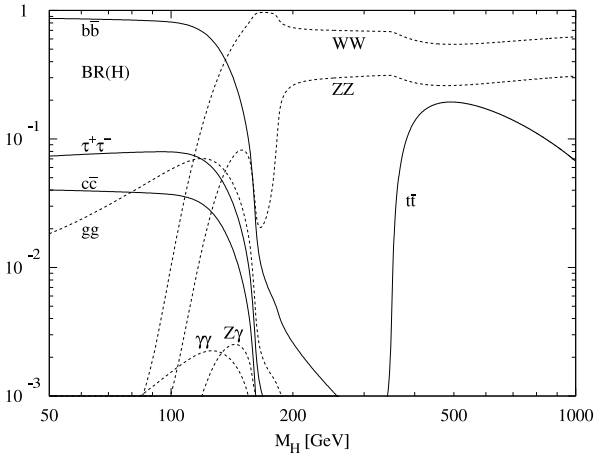

Fig. 3: Higgs decay branching ratios for various channels as functions of M_H

5.1 Signal signature

Although the Z bosons from the Higgs can decay to e^+e^-, $\mu^+\mu^-$, $\tau^+\tau^-$, $q\bar{q}$ or $\nu_{e/\mu/\tau}\bar{\nu}_{e/\mu/\tau}$, the prefered final state generally includes electrons and/or muons, since these provide a much cleaner signature. A Feynman representation of the $H \to ZZ \to 4l$ process is shown in Fig. 4. In principle, each flavour contributes to the loop, but as the Higgs couplings to fermions are proportional to the fermion masses, the top quark is responsible for the dominant contribution.

5.2 Theoretical framework

To compute the decay rate for the process it is necessary to use the corresponding Feynman rules, deduced from the Standard Model Lagrangian. Here, this corresponds to the right-hand side ($H \to ZZ$) vertex in Fig. 4. The complex amplitude is given by

$$i\mathcal{M} = 2i\frac{m_Z^2}{v} g^{\mu\nu} \varepsilon_\mu(k_1)\varepsilon_\nu(k_2) \,, \tag{11}$$

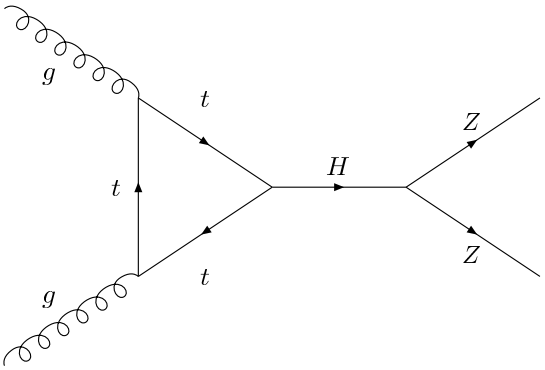

Fig. 4: A Feynman representation of Standard Model Higgs production via gluon fusion, and subsequent decay to two Z bosons

which implies

$$|\mathcal{M}|^2 = 4\frac{m_Z^4}{v^2}\varepsilon_\mu(k_1)\varepsilon_\nu^*(k_1)\varepsilon^\mu(k_2)\varepsilon^{\nu*}(k_2)\ , \tag{12}$$

where $\varepsilon_\mu(k_1)$ is the polarization vector of the outgoing particle with 4-momentum k_1, and v is the vacuum expectation value of the Higgs field.

When one is not interested in measuring the polarization of the outgoing Z's, it is useful to exploit the relationship (valid for massive gauge vectors)

$$\sum_{pol}\varepsilon_\alpha^*(k)\varepsilon_\beta(k) = -g_{\alpha\beta} + \frac{k_\alpha k_\beta}{m^2}$$

where m is the mass of the vector boson. After some algebra we obtain

$$\sum_{pol}|\mathcal{M}|^2 = 4\frac{m_Z^4}{v^2}\left[2 + \frac{(k_1\cdot k_2)^2}{m_Z^4}\right]. \tag{13}$$

Using the general considerations of Section 2 and working in the centre-of-mass frame one can show that

$$\sum_{pol}|\mathcal{M}|^2 = 4\frac{m_Z^4}{v^2}\left[3 - \frac{m_H^2}{m_Z^2} + \frac{m_H^4}{4m_Z^4}\right]. \tag{14}$$

Finally, taking into account that the Higgs is decaying into two identical particles, and setting $v^2 = m_H^2/2\lambda^2$), we arrive at

$$\Gamma = \frac{\lambda}{2\pi}\frac{m_Z^4}{m_H^2}\sqrt{m_H^2 - 4m_Z^2}\left[3 - \frac{m_H^2}{m_Z^2} + \frac{m_H^4}{4m_Z^4}\right]. \tag{15}$$

From this, it can be seen that $m_H \geq 2m_Z \sim 180$ GeV for the decay to occur. In these calculations, it was assumed that both Z bosons were on-shell—a justified simplification considering that the off-shell contribution for the process is heavily suppressed by the propagators for the virtual particles. Indeed, if we return to Fig. 3 we see a sharp increase in the $H \to ZZ$ branching ratio at around 180 GeV.

5.3 Background

The dominant background for the $H \to ZZ \to 4l$ process comes from the irreducible $ZZ \to 4l$ continuum over the full mass range. For smaller Higgs masses, where one of the Z bosons is off-shell, the leptons have a lower p_T [7]. In this region, backgrounds from $Zb\bar{b} \to 4l$ and $t\bar{t} \to W^+W^-b\bar{b} \to 4l$ are also significant, but reducible.

Both these backgrounds contain $b\bar{b}$ pairs which can decay to leptons, thus faking the signal. However, leptons from the signal should be isolated, whereas those from b-daughters are often accompanied by hadronic jets. Placing isolation requirements on the electrons and muons should help to reduce the number of b-daughters which are reconstructed as coming from the Z decay.

A veto on events with a significant amount of missing transverse energy can help to reduce the contribution from leptonic W decays (from top quark decays) since these are always accompanied by a neutrino.

6 Analysis cuts and potential pitfalls

To claim a discovery of rare decays like $B_s \to \mu^+\mu^-$ and $H \to ZZ$, a statistically significant peak in the mass distribution above the expected background must be identified. The reduction of background contributions over the full range of the mass interest is therefore crucial. Where the initial mass is known, the kinematic parameters of the decay are fully constrained and analysis cuts should not be based on the kinematic variables since this can further constrain the mass peak without necessarily improving the signal-to-background ratio. Instead, one should aim to base initial selection cuts on non-kinematic variables. For $B_s \to \mu^+\mu^-$ such cuts may be based upon

i) B_s impact parameter b or impact parameter significance (see Fig. 5).
ii) Angle between B_s momentum and the direction of primary vertex (PV) to secondary vertex (SV).
iii) To reduce combinatorial background, muons should come from the same SV, so that the mismatch x between the expected decay length of the B_s and the SV should be small (e.g., cut on secondary vertex χ^2).
iv) The angular distribution of the muons in the rest frame of the B_s should be isotropic. If Θ is the angle between the PV and SV direction and one-muon momentum this implies that the $\cos(\Theta)$ distribution is flat.

All cuts (direct or indirect) on the muon momentum and energy should be avoided as these will bias the mass distribution. A cut on momentum will remove background that falls outside of the mass peak, but not within. The ratio between the tails and the amplitude of the mass distribution would therefore appear to be improved, but any background that happens to be kinematically similar to the signal is not removed.

Cuts on the opening angle of the muons in the rest frame of the B_s will affect the signal in the same way. This will remove background that is not decaying with an opening angle of 180 degrees, but one must bear in mind that all two-body decays will behave in the same manner. Again, we observe that backgrounds kinematically similar to the signal (e.g., B_s to K^+K^-) are not removed, thus artificially enhancing the peak in the invariant mass distribution. The same reasoning can be applied to $H \to ZZ$ analysis cuts.

7 Conclusions

We have worked out the general form of two-body decays, and applied it to the study of two important processes expected to be observed at the LHC. Owing to energy–momentum conservation, the kinematical magnitudes of the final states are fully fixed, depending exclusively on the mass of the particles and the energy of the initial particle.

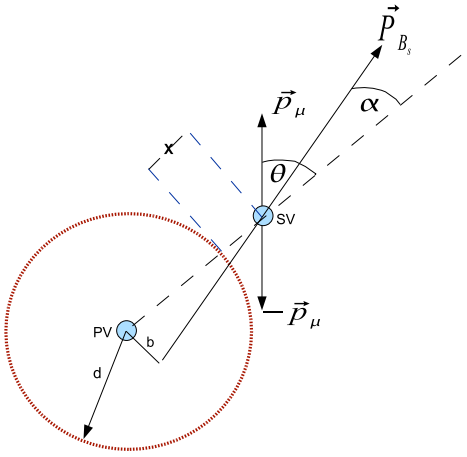

Fig. 5: Kinematics in the rest frame: where impact parameter b = distance of B_s momentum to primary vertex (PV), α = angle between B_s momentum and the direction of PV to secondary vertex (SV), d = decay length of B_s, Θ = angle between the PV and SV direction and one muon momentum, and x = mismatch between SV and d (B_s decay length)

One of the most important characteristics of these processes is their angular dependence when observed in the centre-of-mass frame. In this scenario—when the emission of decay particles occurs back-to-back—severe constraints are imposed on the potential for cleanly separating the signal from background. In particular, one should note that any cut that depends on either the energies or the 3-momenta of the final-state particles has the potential to bias results. Furthermore, even when secondary decays take place, the detected decay products must be isotropically distributed in the centre-of-mass frame.

Not taking into account these simple considerations when imposing cuts may mean that the wrong conclusions can be drawn, due to possible enhancement of background noise in the relevant region of observation.

References

[1] M.E. Peskin and D.V. Schroeder, An Introduction to Quantum Field Theory (Addison-Wesley, Reading, USA, 1995), p. 842.

[2] M. E. Albrecht, W. Altmannshofer, A. J. Buras, D. Guadagnoli, and D. M. Straub, Challenging SO(10) SUSY GUTs with family symmetries through FCNC processes, arXiv:0707.3954v3 [hep-ph].

[3] http://www-cdf.fnal.gov/physics/new/bottom/060316.blessed-bsmumu3/ and CDF public note 8176.

[4] D. Martinez, J. A. Hernando, and F. Teubert, LHCb potential to measure/exclude the branching ratio of the decay $B_s \to \mu^+\mu^-$, CERN-LHCB-2007-033 (2007).

[5] ATLAS Collaboration, ATLAS Detector and Physics Performance Technical Design Report, CERN/LHCC/99-14 (1999).

[6] ATLAS Collaboration, Expected Performance of the ATLAS Experiment, Detector, Trigger and Physics, CERN-OPEN-2008-020 (2008).

[7] A. D'Orazio on behalf of the ATLAS Collaboration, Standard Model Higgs search in the 4-lepton final state with ATLAS, Proceedings of 'Physics at the LHC 2008', CERN-ATL-PHYS-PROC-2009-019 (2009).